GOSPODARKA SUROWCAMI MINERALNYMI – MINERAL RESOURCES MANAGEMENT

2023 Volume 39 Issue 4 Pages 157–180

DOI: 10.24425/gsm.2023.148164

RAFAŁ MISA[1]

Knothe's theory parameters – computational models and examples of practical applications

1. Introduction and mathematical model

For over seventy years (Jiang et al. 2006; Malinowska et al. 2020; Polanin et al. 2019), Knothe's theory, published in 1951 (Knothe 1951), has been successfully improved and practically applied in various areas, including coal mining (Kowalski et al. 2021; Strzałkowski 2022), salt mining (Blachowski 2016; Hejmanowski and Malinowska 2017) and ore exploitation (Niedojadło et al. 2023; Zhang et al. 2020).

Geometric integral methods as an example of influence function methods, especially Knothe's method, have been successfully used in Europe, e.g. in Poland, Germany, Czech Republic, Slovakia, Great Britain and Spain (Díez and Álvarez 2000; Jirankova et al. 2020;

✉ Corresponding Author: Rafał Misa; e-mail: misa@imgpan.pl

[1] Strata Mechanics Research Institute, Polish Academy of Science, Kraków, Poland; ORCID iD: 0000-0003-3339-8839; Scopus ID: 56866167400; Researcher ID: E-8634-2018; e-mail: misa@imgpan.pl

Kwinta et al. 1996; Marcak and Pilecki 2019; Sedlák et al. 2018; Sroka et al. 2015). Knothe's theory was also adapted to mining conditions in the United States and Canada (Karmis et al. 1990; Szostak-Chrzanowski et al. 2006). This theory is still successfully used in Australia and Asia, e.g. China, Vietnam, Thailand, India and Iran (Asadi et al. 2004; Han et al. 2019; Jiang et al. 2020; Kapp 1980; Sheorey et al. 2000). In the following considerations, a generalization of Knothe's Theory was utilized, which involves analyzing the interaction of a complex element. The size of such a complex element is determined in order to create a basin on the surface of the terrain that closely resembles a Gaussian function. By using such a solution, it is possible to accurately consider the shape (geometry) of the exploited deposit. Among other factors, the influence of depth and thickness is taken into account in such cases; also included is the inclination of the adjacent rock mass, its anisotropy, and the progress of mining over time through accurate recording of the element selection time (Hejmanowski 2001; Sroka 1984; Sroka et al. 1988). The general scheme of dependencies is presented in Figure. 1.

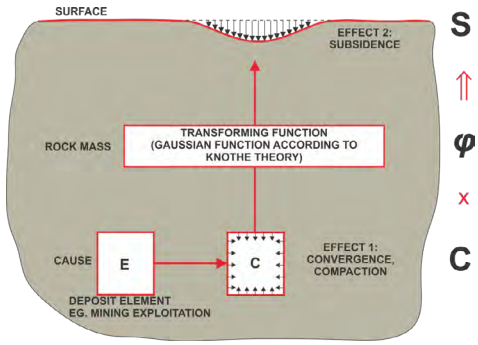

Fig. 1. Conceptual diagram of the computational model (Sroka et al. 2018a)

Rys. 1. Schemat ideowy modelu obliczeniowego

The two-stage diagram was used to illustrate the computational idea, which enables a better understanding of the concept and serves as a generalized scheme for various forms of mining. In the presented conceptual computational model, the cause is human mining activity associated with: the extraction of solid, liquid and gas resources; the construction of caverns for oil and gas storage; the exploitation of geothermal deposits for "heat" extraction; inundation by raising the water level in mining areas; areas of rock mass disintegration due to previous mining operations. The first consequence is the convergence of the selected cavity within the complex element during the block caving mining of coal deposits or the pillar-room mining of sulfur or metal ore deposits, the compaction of a porous fluid deposit caused by a decrease in pore pressure, the convergence of salt caverns, volume change due to the cooling of rock mass during "heat" exploitation, or vertical expansion (decompaction) of post-mining disintegrated porous areas due to increased pore pressure caused by rising

water levels in mining areas. The second consequence is the deformation of the rock mass and the surface terrain.

Assuming that the influence function takes the form of a Gaussian function (Figure 2) in the parameterization given by Knothe (Knothe 1951), for a complex element, we obtain (1):

$$s(r,t) = \frac{a \cdot K(t-\Delta t)}{R^2} \exp\left(-\pi \frac{r^2}{R^2}\right) \tag{1}$$

- a – the vertical scale parameter, which is a subsidence coefficient dependent on the mining technology and roof protection method, representing the proportion of the expected subsidence basin volume to the volume change in the reservoir zone caused by convergence or compaction (consequence 1) – also referred to as the exploitation coefficient, describing the actively settling part of the post-mining void, and is also known in the literature as the surface subsidence coefficient, subsidence coefficient and roof control coefficient (dimensionless value);
- r – the distance from the computational point to the complex element;
- t – time;
- $K(t)$ – the volume change of the complex element over time t;
- $a \cdot K(t - \Delta t)$ – the volume of the subsidence basin on the surface at time t;
- Δt – the time shift (delay) caused by the delayed interaction of the adjacent rock mass;
- R – the radius of main influence range ($R = H \cdot cot\ \beta$), a parameter indicating the spread of mining influences;
- H – the mining depth;
- β – the angle of main influence range (Knothe 1953a).

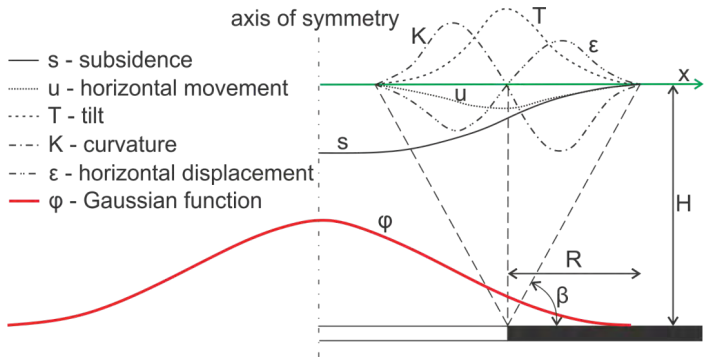

Fig. 2. Idealized distribution of displacements and deformations with the influence function (own work)

Rys. 2. Wyidealizowany rozkład przemieszczeń oraz deformacji wraz z funkcją wpływów

In Knothe's theory, we can generally distinguish four scale parameters, including the relative scale parameters: the vertical scale parameter a, the horizontal displacement parameter λ, the horizontal range scale parameter $cot\beta$, and the time scale parameter c.

2. Subsidence coefficient resulting from mining technology

The method of mining is one of the mining factors that can be used to minimize surface deformations. Among them, full and partial mining can be distinguished. Full mining involves the complete extraction of the seam, while partial mining includes methods such as pillar-and-panel mining or longwall mining. Both full and partial mining can be conducted with or without backfilling the post-mining voids, or with hydraulic or pneumatic stowing.

2.1. Full mining with roof caving

Full mining with roof caving is a frequently utilised coal mining technique, particularly in Polish mining. In this type of mining, the subsidence coefficient is defined as the ratio of the volume M of the resulting subsidence basin to the volume V of the extracted deposit:

$$a = \frac{M}{V} \tag{2}$$

- M – the volume of the subsidence basin;
  V – the volume of the extracted deposit.

In the professional literature, the subsidence coefficient is also defined as the ratio of the maximum subsidence of the full or overfilled basin to the average thickness of the mined seam.

$$a = \frac{s_{max}}{g} \tag{3}$$

- s_{max} – maximum subsidence of the basin;
  g – thickness of the mined seam.

If we take a value of a = 0.8, it indicates that only 80% of the chosen volume results in a subsidence basin, while the remaining 20% creates relaxation zones in the rock mass. The contraction and compaction of this zone depend on the depth of mining, i.e. the pressure exerted by the overlying rocks. For greater depths, the value of this coefficient is higher. Moreover, in the case of multi-seam mining, the activation of "old works" often occurs, which

refers to additional subsidence caused by the extraction of a seam located below previously mined seams. In such cases, the value of the subsidence coefficient can reach 1.0. This has been confirmed by, among other things, *in-situ* observations in the German Prosper Haniel mine in Bottrop. For predictive calculations, the value of parameter a is then assumed within the range:

$$0.9 \leq a \leq 1.0$$

2.2. Full mining with backfilling

One of the methods to minimize deformations caused by underground mining, in addition to partial mining, can be the use of pneumatic or hydraulic backfilling. By employing backfilling, waste disposal is facilitated, fire prevention is ensured, and the exploitation of thick seams becomes possible while minimizing the impact on the surface.

One way to determine the mining coefficient is through the analysis of geodetic measurements of deformations in a given area. In cases where appropriate geodetic deformation measurement results are not available, it is recommended to adopt the value of the coefficient from Table 1 (GIG 1996) assuming typical mining-geological conditions for coal mining and assuming a parameter of $cot\beta = 0.5$ ($tan\beta = 2.0$). For copper mines in the Legnica-Głogów Copper District (LGOM), the value of $cot\beta$ is taken as 0.760 ($tan\beta = 1.3$).

It should be noted that various natural and technical factors influence the values of mining coefficients, and for hydraulic backfill, the following natural factors are the most im-

Table 1. Compilation of mining coefficient values for coal mining conditions in Poland (GIG 1996)

Tabela 1. Zestawienie wartości współczynnika eksploatacji dla warunków zagłębi węglowych w Polsce

Method of selected space closure – mining system	The value of the coefficient
Roof caving	0.7–0.85*
Dry backfill – full with supplied material	0.5–0.6
Pneumatic dry backfill	0.4–0.5
Hydraulic backfill with sand	0.15–0.25
Hydraulic backfill with crushed stone	0.3
Partial mining with 50% strip mining and hydraulic backfill	0.02–0.03
Partial mining with 50% strip mining and roof caving	0.1

* Higher values should be assumed for multiple mining operations.

portant: mining depth, tilt and thickness of the seam, and the geological structure of the adjacent strata. Mining technology can be considered to be the most significant technical factor influencing the value of the mining coefficient *a*.

2.3. Room-and-pillar mining with and without backfill

For room-and-pillar mining, the value of the mining coefficient depends on factors such as:

- the load-bearing capacity of the remaining pillars,
- the strength of the roof rocks,
- the width of the mining excavations,
- the depth of the planned mining operation,
- the deposit utilization coefficient.

In the context of analyzing, for example, the values of mining coefficients for room-and-pillar mining in the case of copper mining in KGHM mines (Poland), we can mention the study by Sroka and Hejmanowski from 1996 (Sroka and Hejmanowski 1996), which relates the value of this coefficient to the strata loss coefficient η_s (Tajduś et al. 2012).

$$a(\eta_s) = a_0 (1 - \eta_s)^{\omega} = a_0 \eta^{\omega} \tag{4}$$

- a_0 – is the subsidence coefficient dependent on the adopted excavation closure system for full mining;
- η_s – is the strata loss coefficient ($\eta_s = 1 - \eta$);
- η – is the deposit utilization coefficient;
- ω – is the power coefficient, with a value ranging from 1.5 to 2.0.

The above formula is purely empirical in nature.

For room-and-pillar systems in KGHM copper mines, the following values of the mining coefficient are typically assumed:

- for caving systems, $a = 0.5$;
- for systems with hydraulic backfill, $a = 0.2$.

Recent verifications of this parameter based on in-situ subsidence measurements indicate that the values of this coefficient have much wider ranges and are dependent on the increasing degree of deposit utilization and the growing depth of mining operations. The ranges of subsidence coefficient values described by Niedojadło (Niedojadło 2008) are expressed by the following inequalities:

- for caving mining: $0.45 \leq a \leq 0.80$;
- for mining with hydraulic backfill: $0.20 \leq a \leq 0.35$.

The mining coefficient is generally also dependent on the value of the large-area deflection of the roof rock panels on the remaining pillars, i.e. the convergence of the roof rocks. In LGOM mines, the following relationship between the convergence rate and the face advance rate can be observed (Figure 3). This relationship is linear, although its exact form may vary depending on the size of the mining field.

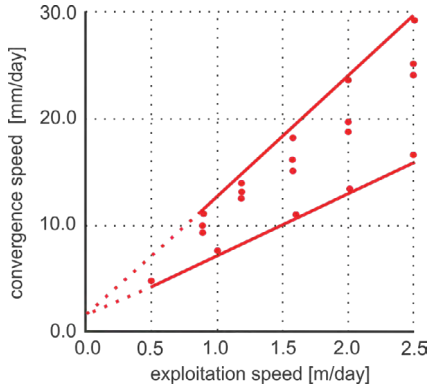

Fig. 3. Relationship between convergence velocity and advancement velocity of the mining front (Hejmanowski 2004)

Rys. 3. Zależność prędkości konwergencji od prędkości postępu frontu eksploatacji

The exploitation coefficient in the case of room-and-pillar mining with backfill is determined based on the results of laboratory and engineering studies. Laboratory tests involve determining the physical and mechanical properties of rocks, including their compressive, shear, and impact strength. Engineering studies involve determining the influence of geotechnical factors, such as stress levels, rock strength and load-bearing capacity, on the subsidence of pillars.

2.4. Salt caverns

In the mid nineteen-eighties, surface subsidence due to convergence liquefied storage caverns in salt formations reached measurable values in Germany. As part of a project funded by the Lower Saxony government, Sroka and Schober (Sroka and Schober 1982) provided a solution based on Knothe's theory (5) regarding the distribution of subsidence above a single cavern (Figure 4).

$$S(r,t) = s_{\max}(t) \cdot \frac{R_r \cdot R_f}{r \cdot h} \cdot \tan\beta \cdot \left[F\left(\frac{r}{R_f}\right) - F\left(\frac{r}{R_r}\right) \right] \tag{5}$$

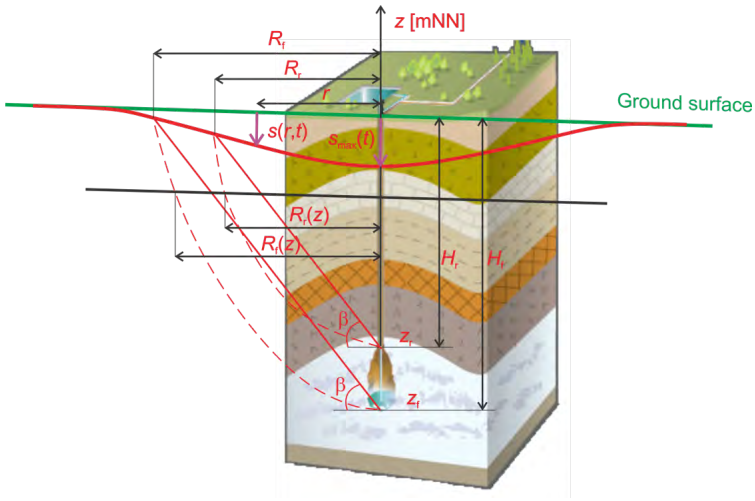

Fig. 4. Subsidence basin above a salt cavern (Tajduś et al. 2021)

Rys. 4. Niecka obniżeniowa nad kawerną solną

where:

$$F\left(\frac{r}{R}\right) = \int_{r/R}^{\infty} \exp\left(-\pi\lambda^2\right) d\lambda \tag{6}$$

$$R_f = H_f \cdot cot\beta, \quad R_r = H_r \cdot cot\beta \tag{7}$$

$S(r,t)$ – a surface point subsidence at time located at a distance from the axis of the cavern;
$S_{max}(t)$ – maximum subsidence at time t;
h – height of the cavern;
R_r – radius of the main influence range measured from the cavern roof;
R_f – radius of the main influence range measured from the cavern floor;
H_r – the cavern roof depth;
H_f – the cavern floor depth.

The detailed solution regarding the volume of the subsidence basin $M(t)$ was presented, inter alia, in the work of (Tajduś et al. 2021).

Typical convergence coefficients, characteristic for Epe, one of the German cavern fields, (corresponding to the percentage annual volume loss of the cavern), are presented in Table 2. The importance of the convergence rate of gas caverns for the observed subsidence above these caverns is noticeable in the Table 2.

The value $S_{max}(t)$ of also depends on the shape of the cavern and the geometric convergence model, including (Hartmann 1984; Haupt et al. 1983; Sroka et al. 2017). Comparative

Table 2. Typical annual convergence rates in Epe (Meyer et al. 2019)

Tabela 2. Typowe roczne wskaźniki konwergencji w polu Epe

Cavern filled with	Convergence ξ (%/year)
Brine	0.5–0.9
Oil	0.2–0.3
Natural Gas	0.6–2.5

calculation results lead to the conclusion that the maximum subsidence can be accurately approximated using the following equation (8):

$$S_{\max}(t) = \frac{a \cdot K(t - \Delta t)}{R^2} \tag{8}$$

Despite the necessary geometric and physical idealizations regarding the cavern geometry, convergence behavior, and usage phases, comparative calculations performed for the EPE cavern field fully confirmed the usefulness of the presented solution (Hengst 2014).

2.5. Fluid deposits: gas, oil and water from aquifers

According to the presented computational scheme for an element of a fluid deposit, the corresponding elementary basin on the ground surface can be described by the Knothe's theory equation (1). In this case, the variable $K(t)$ represents the volume compaction of the porous element of the fluid deposit at time .

The horizontal dimension of the deposit element, which has a square shape, should not exceed the value of $L \leq 0.1 \cdot R$ (Sroka 1984). A crucial stage is the division of the exploited fluid deposit into elements with parameters:

- coordinates x, y, z;
- depth H;
- thickness of the reservoir layer g;
- porosity η;
- stiffness modulus E_s;
- pore pressure for different time moments $p(t)$.

This discretization of the deposit (Figure 5) enables the complete consideration of the spatial shape of the deposit and its spatial distributions of properties necessary for the calculation process.

According to the cause-and-effect model, when the pressure in the pores of porous reservoir rocks decreases, they become more compacted, resulting in surface subsidence. This

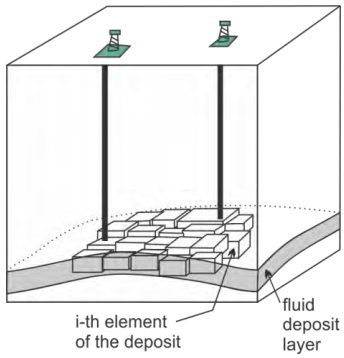

Fig. 5. Scheme of discretization of a fluid deposit into reservoir elements (Sroka and Tajduś 2009)

Rys. 5. Schemat dyskretyzacji złoża fluidalnego na elementy złożowe

compaction also leads to the creation of an elementary basin, described by equation (9) in the case of a deposit element (as shown in Figure 6).

$$s_{j,i}(r,t) = \frac{\Delta g_i(t) \cdot L^2}{R_{j,i}^2} \exp\left(-\pi \frac{r_{j,i}^2}{R_{j,i}^2}\right) \tag{9}$$

- $\Delta g_i(t)$ – absolute vertical compaction of the i-th element at time t;
- $s_{j,i}(r,t)$ – subsidence of the j-th surface point caused by the compaction of the i-th reservoir element;
- $r_{j,i}$ – distance of the j-th computational point from the i-th reservoir element.

The total subsidence of any surface point is calculated assuming linear superposition, i.e. as the sum of point depressions caused by individual reservoir elements:

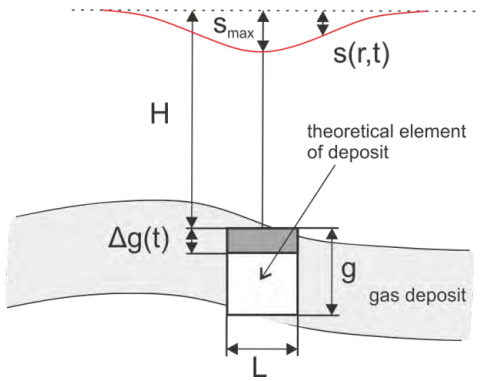

Fig. 6. Surface subsidence above the exploitation of the i-th deposit element (Zimmermann et al. 2018)

Rys. 6. Obniżenie terenu powstające nad eksploatacją i-tego elementu złoża

$$s_{j,i} = \sum_{i=1}^{i=N} s_{j,i} \tag{10}$$

- N – number of reservoir elements.

For reservoir rocks in the form of sandstone with porosity up to 20%, reservoir compaction can be estimated using Biot's consolidation theory:

$$\Delta g_i(t) = C_{mi}\left[p_0 - p_i(t)\right] \cdot M_i \tag{11}$$

$$C_{mi} = \frac{\lambda_i(\eta)}{E_{si}} \tag{12}$$

- C_{mi} – compaction coefficient of the i-th reservoir element, representing vertical deformation of the deposit per unit pressure change;
- p_0 – initial pressure;
- $p_i(t)$ – pressure in the i-th reservoir element at time t;
- M_i – poroelasticity of the porous deposit;
- E_{si} – stiffness modulus of the reservoir rocks;
- $\lambda_i(\eta)$ – Biot coefficient dependent on the type of reservoir rocks and their porosity (Nowakowski and Nurkowski 2021).

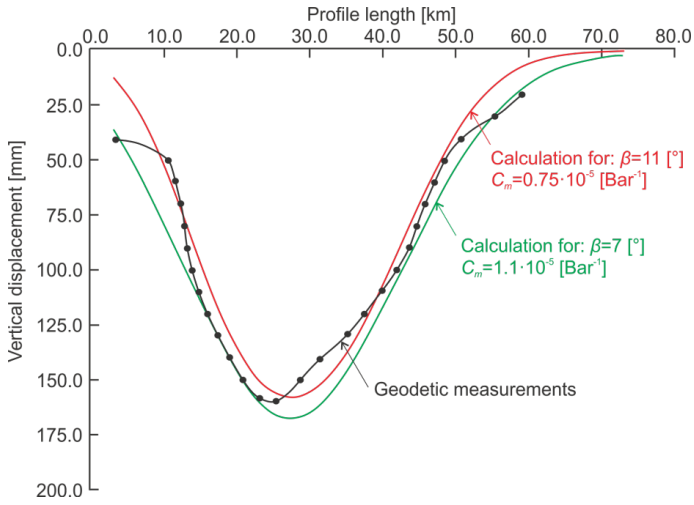

Fig. 7. Comparison of the measured and theoretically calculated subsidence basin for the Groningen gas field (as of 1987) (Sroka et al. 2018a)

Rys. 7. Porównanie niecki pomierzonej i obliczonej teoretycznie dla złoża gazu w Groningen (stan na 1987 rok)

The compaction coefficient's value varies based on the type of rock and its deformation parameters. The literature often provides relationships between the value of the compaction coefficient and porosity (Schutjens et al. 1995; Teeuw 1973).

Figure 7 shows a comparison between the theoretically calculated and measured subsidence basin profile for the Groningen gas field in the Netherlands (Sroka and Schober 1990).

2.6. Flooding of mines

After the deactivation of dewatering pumps, the process of flooding occurs naturally through the influx of water from adjacent rock strata, leading to a gradual rise in the level of mine water. It is assumed that the increase in pore pressure in the consolidated caved zone, caused by the rise in mine water level, results in the vertical expansion of this zone and is directly responsible for the observed surface uplift. The pressure also increases in the disintegrated rock zone, causing a change in the volume of this zone (Dudek et al. 2022, 2020; Dudek and Tajduś 2021; Sroka et al. 2021; Tajduś et al. 2023). This volume change in an element of the disintegrated zone can be described by the equation:

$$K(t) = d_m \cdot \Delta p(t) \cdot \lambda \cdot M \cdot L^2 \tag{13}$$

- λ – relative height of the disintegrated rock element (e.g. $\lambda = 3$ corresponds to an absolute height three times the thickness of the depleted deposit);
- $\Delta p(t)$ – increase in pore pressure in the disintegrated zone, dependent on the height of the water column above this zone;
- d_m – expansion coefficient.

In 2012, Sroka and Preusse conducted a surface uplift forecast for the Königsborn mine area (Ruhr District – Germany). The uplift prediction analysis was verified (Preusse and Sroka 2015) through field measurements in 2015 (Figure 8), confirming the accuracy of the applied methodology (Sroka and Preusse 2009a).

Table 3 presents exemplary values of characteristic parameters d_m, λ and γ_w for selected areas of hard coal. γ_w represents the critical angle of mine water uplift used in calculations for the Ruhrkohle method.

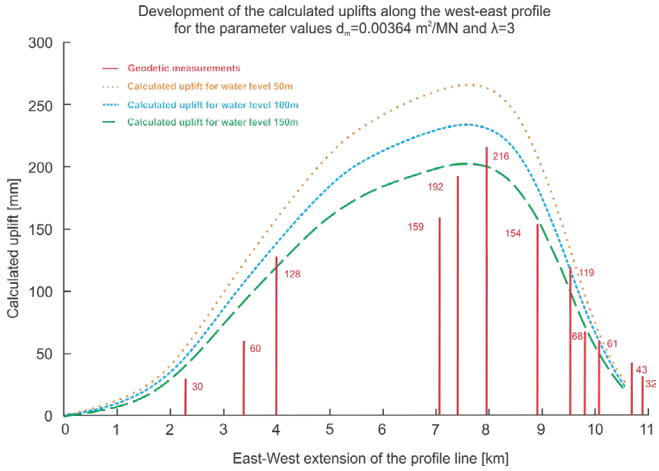

Fig. 8. The uplift development along the east-west profile for a sample coal mine (Preusse and Sroka 2015)

Rys. 8. Rozwój wypiętrzeń wzdłuż profilu z zachodu na wschód dla przykładowej kopani węgla kamiennego

Table 3. Comparison of characteristic values d_m, λ and γ_w for selected areas of hard coal (Sroka et al. 2022)

Tabela 3. Zestawienie wartości charakterystycznych d_m, λ i γ_w dla wybranych okręgów węgla kamiennego

Coalfield	d_m (m²/MN)	λ	$d_m \cdot \lambda$ (m²/MN)	γ_w (gon)
Südlimburger Revier (Pöttgens 1985)	$0.350 \cdot 10^{-2}$	4	$1.40 \cdot 10^{-2}$	–
Ibbenbüren/Westfeld (Goerke-Mallet 2000)	$0.460 \cdot 10^{-2}$	3	$1.38 \cdot 10^{-2}$	–
Erkelenzer Revier/Sophia Jacoba (Sroka and Preusse 2009b)	$0.265 \cdot 10^{-2}$	4	$1.06 \cdot 10^{-2}$	$\frac{7–15}{\gamma_w} = 12$
Ruhrrevier/Königsborn (Preusse and Sroka 2015)	$0.364 \cdot 10^{-2}$	3	$1.092 \cdot 10^{-2}$	12

3. Evolution of the main influence angle range

The main influence angle range β is a characteristic quantity in Knothe's theory (Knothe 1953b) that describes the physico-mechanical properties of the rock mass undergoing deformation. *Cot*β represents the horizontal extent of the main influences relative to the mining depth.

The initial geometric-integral solutions (Bals 1931; Keinhorst 1925; Schmitz 1923) introduced the concept of the angle of refraction, which indicated that deformation indicators outside the boundaries of this angle were zero on the terrain surface.

3.1. Knothe method and Ruhrkohle method

As previously mentioned, Knothe's theory (Knothe 1951) has found significant application in the description of the effects of broadly understood mining both in Poland and worldwide, while the Ruhrkohle method based on it is used in German mining (Ehrhardt and Sauer 1961).

Both computational methods rely on the influence function, which is parameterized differently as a Gaussian function. The different parameterization arises from the different descriptions of the so-called influence range angle. Utilizing the provided relationship between the main angles (γ and β) of the Ruhrkohle and Knothe's methods given below (14), the same results are obtained regardless of the chosen computational method.

$$\pi \cdot tan^2\beta = k \cdot tan^2\gamma \tag{14}$$

- β – angle of the main influences according to Knothe's theory;
- γ – angle of the boundary influences according to the Ruhrkohle method;
- k – the Ruhrkohle method constant ($k = -\ln 0.01 = 4.60517...$).

In contrast to the methods mentioned earlier by Schmitz, Keinhorst and Bals, these methods are characterized by non-zero deformation indicator values at the boundary determined by the limiting value of the influence angle. One such example is the Ruhrkohle method, in which the relative subsidence at the boundary of the influence angle is 0.1% of the maximum subsidence, and the tilts and horizontal displacements are 1.0% of their maximum values, while the curvatures and strains at the boundary of the main influence angle contribute 5.0% of their maximum values (Sroka 2011).

The values of displacements and deformation indicators at the edge of the main influence angle on the ground surface in the classical Knothe method have values of 0.6% of the maximum settlement for subsidence and 4.3% of their maximum values for tilts and strains (Knothe 1984).

Example empirical results regarding the values of the main influence angle range β for German cavern fields are presented in Table 4.

Assuming an average mining depth of approximately 700 m, the relative parameter of the main influence range in the Upper Silesian Coal Basin falls within the range: $0.385 \leq cot\beta \leq 0.588$ ($2.60 \geq tan\beta \geq 1.70$). Therefore, it can be assumed that the angle of the main influence range varies within the value range of $59.53° \leq tan\beta \leq 68.96°$. However, for mining areas of the LGOM mines, the parameter of the main influence range falls within the range of $0.588 \leq cot\beta \leq 0.714$ ($1.70 \geq tan\beta \geq 1.40$), and in accordance with this, the values of the angle of the main influence range should fall within the range of $54.46° \leq \beta \leq 59.53°$ (Konopko and Bukowska 2008).

Table 4. Example empirical values of the main influence angle range for German cavern fields

Tabela 4. Przykładowe wartości empiryczne kąta zasięgu wpływów głównych dla niemieckich pól kawern

No.	Author/Year	β (°)
1	Hartmann (1984)	27.0–29.7
2	Sroka (1984)	30.0
3	Schober et al. (1987)	30.0
4	Quasnitza (1988)	35.1
5	Düsterloh (1993)	22.5–25.2
6	Eickemeier (2005)	34.8
7	BGR-Hannover (2016)	approx. 26.0
8	Sroka et al. (2017)	34.0

4. Knothe's time-related solution

The assumption of the proportionality between the subsidence rate of a point at a specific time t and the difference between the final subsidence that the point can undergo due to the selected elementary coal seam and the subsidence value of point $s(t)$ at any given moment, formed the basis of Knothe's proposed solution (Knothe 1953b) (15).

$$\dot{s}(t) = \frac{\partial s(t)}{\partial t} = c\left[s_e - s(t)\right] \tag{15}$$

- $\dot{s}(t)$ – subsidence rate (velocity);
- s_e – final subsidence (established, asymptotic);
- c – subsidence-rate coefficient representing the average relative rate of influence transfer by the surrounding rock mass with respect to the underground mining depth – rock mass properties affect the value of this coefficient;
- $s(t)$ – actual, instantaneous subsidence value.

By solving the following equation (16) with the initial condition $s(t = 0) = 0$, we obtain:

$$s(t) = s_e\left[1 - \exp(-ct)\right] = s_e f(t) \tag{16}$$

- $f(t) = 1 - \exp(-ct)$ – the so-called time function.

Knothe's solution presented the starting point for numerous theoretical and practical studies on the dynamics of mining influence (Dżegniuk and Sroka 1978; Schober and Sroka

1983; Trojanowski 1973, 1970) and (Cheng et al. 2021; Lian et al. 2011; Zhang et al. 2020). In 1974, Sroka (Sroka 1974) stated in his doctoral thesis that the main cause of damage to structures is the excessive speed (dynamics) of mining operations. Based on several years of research, Hejmanowski and others (Hejmanowski et al. 1997) confirmed that the dynamic effects of rapidly advancing mining faces are a fundamental threat to surface structures. They suggested the following elements to minimize the harmful impact of mining dynamics:

- adjusting the mining speed and duration of mining breaks to the resistance of protected surface structures;
- ensuring a uniform advancement of the mining face while avoiding sudden and significant changes in speed;
- applying a reduction in the length of mining breaks, assuming that continuous mining is optimal, preferably seven days per week.

5. Parameter of horizontal displacement λ

The fundamental indicator of surface deformation describing the risk to building structures is horizontal displacement. Assuming the premise of Awierszyn (Awierszyn 1947) and the formulas of Knothe's theory (Knothe 1951), Budryk (Budryk 1953, 1952) provided the following method for calculating the standard value of the coefficient , called the coefficient of horizontal displacement or the coefficient of horizontal deformation:

$$B = \frac{R}{\sqrt{2\pi}} = 0.40 \cdot R \tag{17}$$

A comprehensive description of the development of previous research results regarding the magnitude of the coefficient B and parameters of horizontal displacement can be obtained from several publications (Głąbicki et al. 2020; Knothe and Sroka 2010; Niedojadło et al. 2014; Puniach et al. 2023; Tajduś 2015). They mainly relate to the relationships described by the formula:

$$B = \lambda \cdot R \tag{18}$$

For both the exploitation of fluid deposits and for salt cavern fields, when analyzing measurements of rock movements (mainly horizontal displacements on the surface), Sroka et al. (Sroka et al. 2018b) noted that the value of the obtained coefficient of horizontal deformation B is greater compared to the value traditionally given by Budryk. In his doctoral thesis, Quasnitza (Quasnitza 1988) provides an equation for calculating the value of this coefficient for one of the German salt cavern fields (Etzel):

$$B = 1.0 \cdot R \pm 0.1 \cdot R \tag{19}$$

Sroka et al. (Sroka et al. 2018b) provided a formula (20) which is identical to the formula given by Drzęźla (Drzęźla 1989) for $n = 0.665$. The value of the coefficient λ (for $B = \lambda \cdot R$) depends on three quantities: the angle of influence range β; the Poisson's ratio ν of the near-surface soil layer; the value of the boundary surface coefficient of influence in the rock mass .

$$\lambda = \frac{n}{2\pi} \cdot \frac{1-\nu}{\nu} \cdot \cot\beta \tag{20}$$

This formula can be successfully used to calculate surface deformations in the case of open-pit mining in the salt rock mass, deformations caused by cavern convergence for storage energy resources and deformations during the exploitation of fluid deposits.

Witkowski et al. (Witkowski et al. 2021) utilized the established Knothe's theory, which relies on a geometric integral model, along with the Multi-Temporal InSAR technique using Sentinel-1 data. They investigated a novel method for calculating the horizontal strain tensor. The new approach was demonstrated and validated through a case study of an underground copper mine (LGOM) in Poland. This involved decomposing satellite radar interferometry observations into vertical and azimuthal displacements in the look direction.

Conclusions

The issue of forecasting the impacts of mining operations on the surface and on objects located in mining areas remains relevant in practically all active or closing mining facilities, not only in Europe but also in other continents. The accuracy of the calculations largely depends on the adopted model and the correctness of the input parameters. This work characterized the parameters of Knothe's theory necessary for the spatiotemporal description of subsidence and other deformation indicators. Several examples of practical application were presented, demonstrating that the current use of Knothe's theory is much broader than its classical use in coal mining. The solution for a single element enables consideration of the tilt of adjacent layers, anisotropy, time and convergence distribution near the exploited deposit. Knothe's theory is a universal tool that enables simple and transparent solutions to many issues related to calculations of subsidence and other deformation indicators caused by the extraction of volume from the rock mass due to mining or post-mining activities.

This work was performed in 2023 as a part of statutory works executed at Strata Mechanics Research Institute of the Polish Academy of Sciences in Cracow, funded by the Ministry of Science and Higher Education.

REFERENCES

Asadi et. al 2004 – Asadi, A., Shakhriar, K. and Goshtasbi, K. 2004. Profiling Function for Surface Subsidence Prediction in Mining Inclined Coal Seams. *Journal of Mining Science* 40, pp. 142–146, DOI: 10.1023/B:JOMI.0000047856.91826.76.

Awierszyn, S.G. 1947. Mining-induced rock mass subsidence. Ugletiechizdat.

Bals, R. 1931. Calculation of mining subsidence: Questions and Answers (*Beitrag zur Frage der Vorausberechnung bergbaulicher Senkungen*). *Mitteilungen aus dem Marks.* 42/43, pp. 98–111 (*in German*).

BGR-Hannover, 2016. Prediction of Subsidence and Other Ground Movement and Deformation Parameters for the Etzel Cavern Facility with 99 Caverns (*Prognose der Senkungen und weiterer Bodenbewe-gungen und Bodenverformungsgrößen für die Kavernenanlage Etzel mit 99 Kavernen*) (*Unpublished work, in German*).

Blachowski, J. 2016. Application of GIS spatial regression methods in assessment of land subsidence in complicated mining conditions: case study of the Walbrzych coal mine (SW Poland). *Natural Hazards* 84(2), pp. 997–1014, DOI: 10.1007/s11069-016-2470-2.

Budryk, W. 1952. Calculating the Method of Underground Exploitation Beneath Surface Structures (*Obliczanie sposobu podziemnej eksploatacji pod obiektami na powierzchni*). *Przegląd Górniczy* 7–8, pp. 7–8 (*in Polish*).

Budryk, W. 1953. Determining the Magnitude of Horizontal Ground Deformations (*Wyznaczanie wielkości poziomych odkształceń terenu*). *Archiwum Górnictwa i Hutnictwa* 1(1), pp. 63–74 (*in Polish*).

Cheng et al. 2021 – Cheng, H., Zhang, L., Guo, L., Wang, X. and Peng, S. 2021. A New Dynamic Prediction Model for Underground Mining Subsidence Based on Inverse Function of Unstable Creep. *Advances in Civil Engineering*, pp. 1–9, DOI: 10.1155/2021/9922136.

Díez, R.R. and Álvarez, J.T., 2000. Hypothesis of the multiple subsidence trough related to very steep and vertical coal seams and its prediction through profile functions. *Geotechnical & Geological Engineering* 18, pp. 289–311, DOI: 10.1023/A:1016650120053.

Drzęźla, B. 1989. Description of Programs for Predicting Rock Deformation Due to Mining Operations, Current State of Software (*Opis programów prognozowania deformacji górotworu pod wpływem eksploatacji górniczej, Aktualny stan oprogramowania*). *Zeszyty Naukowe Politechniki Śląskiej, Górnictwo* 165 (*in Polish*).

Dudek, M. and Tajduś, K. 2021. FEM for prediction of surface deformations induced by flooding of steeply inclined mining seams. *Geomechanics for Energy and the Environment* 28, DOI: 10.1016/j.gete.2021.100254.

Dudek et. al. 2020 – Dudek, M., Tajduś, K., Misa, R. and Sroka, A. 2020. Predicting of land surface uplift caused by the flooding of underground coal mines – A case study. *International journal of rock mechanics and mining sciences* 132, DOI: 10.1016/j.ijrmms.2020.104377.

Dudek et. al. 2022 – Dudek, M., Tajduś, K. and Rusek, J. 2022. The land surface deformation caused by the liquidation of the Anna mine by flooding. *Archives of Environmental Protection* 48(1), pp. 100–108, DOI: 10.24425/aep.2022.140549.

Düsterloh, U. 1993 Rock Mechanics Investigations for Proving the Geotechnical Safety of Waste Disposal Caverns. Publication Series, Department of Geomechanics in Mining, Tunnel Construction, and Waste Disposal Technology (*Gebirgsmechanische Untersuchungen zum Nachweis der geotechnischen Sicherheit von Deponiekavernen. Schriftenreihe Abt. Geomech. im Bergbau, Tunnelbau und Deponietechnik*) (*Unpublished work, in German*).

Dżegniuk, B. and Sroka, A. 1978. The rate of advancement of the mining front versus the process of rock mass and surface deformation (*Prędkość postępu frontu eksploatacji górniczej a proces deformacji górotworu i powierzchni*). Kom. Ochr. Teren. Górniczych PAN (*in Polish*).

Ehrhardt, A. and Sauer, A. 1961. Precalculation of Subsidence, Tilt and Curvature Over Extractions in Flat Formations. *Bergbauwissenschaften* 8, pp. 415–428.

Eickemeier, R. 2005. Subsidence forecasts over caverns – A new model (*Senkungsprognosen über Kavernen – Ein neues Modell*) 34. Geomechanik Kolloquium. Leipzig (*in German*).

Głąbicki et al. 2020 – Głąbicki, D., Kopeć, A., Milczarek, W., Bugajska, N. and Owczarz, K. 2020. Determination of vertical and horizontal displacements of mining areas using the DInSAR and SBAS methods. *EGU Gen. Assem. 2020*, DOI: 10.5194/egusphere-egu2020-13856.

GIG 1996 – Główny Instytut Górnictwa 1996. *Determining Protective Pillars for Surface Structures Over Shafts and Ventilation Shafts Within the Boundaries of Underground Areas in Coal Mines* (*Wyznaczanie filarów ochronnych dla obiektów na powierzchni szybów i szybików w granicach obszarów górniczych kopalń węgla kamiennego*). Ser. Instr. 3 (*in Polish*).

Goerke-Mallet, P. 2000. Studies on Space-Relevant Developments in the Ibbenbüren Hard Coal Mining District with Special Consideration of the Interactions between Mining and Hydrogeology (*Untersuchungen zu raumbedeutsamen Entwicklungen im Steinkohlenrevier Ibbenbüren unter besonderer Berücksichtigung der Wechselwirkungen von Bergbau und Hydrogeologie*). RWTH Aachen (*Unpublished work, in German*).

Han et al. 2019 – Han, H., Xu, J., Wang, X., Xie, J. and Xing, Y. 2019. Surface Subsidence Prediction Method for Coal Mines with Ultrathick and Hard Stratum. *Advances in Civil Engineering*, pp. 1–15, DOI: 10.1155/2019/3714381.

Hartmann, A. 1984. A contribution to the monitoring of cavern systems (*Ein Beitrag zur Überwachung von Kavernenanlagen*) PhD Thesis, Technische Universität Clausthall, Clausthal, Germany (*Unpublished work, in German*).

Haupt et al. 1983 – Haupt, W., Sroka, A. and Schober, F. 1983. Convergence models for cylindrical caverns and the resulting ground subsidence (*Die Wirkung verschiedener Konvergenzmodelle für zylinderförmige Kavernen auf die übertägige Senkungsbewegung*) *Das Marks*. 90, pp. 159–164 (*in German*).

Hejmanowski, R. 2001. Prediction of Rock Mass and Ground Surface Deformations Based on the Generalized Knothe Theory for Solid, Liquid, and Gas Resource Deposits (*Prognozowanie deformacji górotworu i powierzchni terenu na bazie uogólnionej teorii Knothego dla złóż surowców stałych, ciekłych i gazowych*). Kraków: MEERI PAS (*in Polish*).

Hejmanowski, R. 2004. Spatiotemporal Description of Rock Mass Deformations Induced by Pillar-Chamber Exploitation of Seam Deposits (*Czasoprzestrzenny opis deformacji górotworu wywołanych filarowo-komorową eksploatacją złoża pokładowego*). Kraków: AGH (*in Polish*).

Hejmanowski et al. 1997 – Hejmanowski, R., Dżegniuk, B. and Sroka, A. 1997. Optimal Mining Rate from the Perspective of Surface Structures and Rock Mass Protection (*Optymalna prędkość eksploatacji górniczej z punktu widzenia ochrony obiektów powierzchni i górotworu*) (*Unpublished work, in Polish*).

Hejmanowski, R. and Malinowska, A.A. 2017. Land subsidence inversion method application for salt mining-induced rock mass movement (*Wykorzystanie metody odwrotnej w estymacji osiadań powierzchni terenu dla złóż soli*). *Gospodarka Surowcami Mineralnymi – Mineral Resources Management* 33(3), pp. 179–200, DOI: 10.1515/gospo-2017-0034 (*in Polish*).

Hengst, G. 2014. Monitoring of the subsidence induced by cavern convergence considering their effects on the ecological context (*Monitoring der durch Kavernenkonvergenz induzierten Bodensenkungen unter Betrachtung ihrer Wirkungen auf die* ökologischen *Zusammenhänge*). [In:] 15. Geokinematischer Tag. Freiberg, pp. 237–251 (*in German*).

Jiang et al. 2006 – Jiang, Y., Preusse, A. and Sroka, A. 2006. Application of Surface Movement and Mine Mining Damage, VGE Verlag (*in Chinese*).

Jiang et al. 2020 – Jiang, Yu., Misa, R., Tajduś, K., Sroka, A. and Jiang, Ya. 2020. A new prediction model of surface subsidence with Cauchy distribution in the coal mine of thick topsoil condition. *Archives of Mining Sciences* 65(1), pp. 147–158, DOI: 10.24425/ams.2020.132712.

Jirankova et al. 2020 – Jirankova, E., Waclawik, P. and Nemcik, J. 2020. Assessment of models to predict surface subsidence in the Czech part of the Upper Silesian Coal Basin – Case study. *Acta Geodynamica et Geomaterialia* 17(4), pp. 469–484, DOI: 10.13168/AGG.2020.0034.

Kapp, W.A. 1980. Study of mine subsidence at two collieries in the southern coalfield, New South Wales. *Australas. Inst. Min. Met. Proc*. (Australia) 276.

Karmis et al. 1990 – Karmis, M., Agioutantis, Z. and Jarosz, A. 1990. Recent developments in the application of the influence function method for ground movement predictions in the U.S. *Mining Science and Technology* 10(3), pp. 233–245, DOI: 10.1016/0167-9031(90)90439-Y.

Keinhorst, H. 1925. *Calculation of Surface Subsidence*. 25 Jahre der Emschergenossenschaft 1900–1925.

Knothe, S. 1951. *The Impact of Underground Mining on the Surface in Terms of the Protection of Located Objects* (*Wpływ podziemnej eksploatacji na powierzchnię z punktu widzenia zabezpieczenia położonych na niej obiektów*) (*in Polish*).

Knothe, S. 1953a. Effect of time on formation of basin subsidence. *Arch. Min. Steel Ind*. 1, pp. 1–7.

Knothe, S. 1953b. A profile equation for a definitely shaped subsidence trough (*Równanie profilu ostatecznie wykształconej niecki osiadania*). *Archiwum Górnictwa i Hutnictwa* 1, pp. 22–38 (*in Polish*).

Knothe, S. 1984. Forecasting the Effects of Mining Operations (*Prognozowanie wpływów eksploatacji górniczej*) (*in Polish*).

Knothe, S. and Sroka, A. 2010. Stochastic Assessment of the Impact of Mining Operations on Civil Structures in the Mining Planning Process (*Stochastyczna ocena wpływu eksploatacji na obiekty budowlane w procesie planowania eksploatacji górniczej*). [In:] III Konferencja Naukowo-Szkoleniowa „Bezpieczeństwo i Ochrona Obiektów Budowlanych Na Terenach Górniczych". pp. 155–173 (*in Polish*).

Konopko, W. and Bukowska, M. 2008. The parameter tanβ as a measure of the rock mass tendency to tremor (*Parametr tgβ jako miara skłonności górotworu do tąpań). Górnictwo i Geoinżynieria* 32(1), pp. 139–152 (*in Polish*).

Kowalski et al. 2021 – Kowalski, A., Białek, J. and Rutkowski, T. 2021. Caulking of Goafs Formed by Cave-in Mining and its Impact on Surface Subsidence in Hard Coal Mines. *Archives of Mining Sciences* 66(1), pp. 85–100, DOI: 10.24425/ams.2021.136694.

Kwinta et al. 1996 – Kwinta, A., Hejmanowski, R. and Sroka, A. 1996. A time function analysis used for the prediction of rock mass subsidence. *Mining Science and Technology*. pp. 419–424.

Lian et al. 2011 – Lian, X., Jarosz, A., Savvedra-Rosas, J. and Dai, H. 2011. Extending dynamic models of mining subsidence. *Trans. Nonferrous Met. Soc. China* 21, pp. 536–542, DOI: 10.1016/S1003-6326(12)61637-9.

Malinowska et al. 2020 – Malinowska, A., Hejmanowski, R. and Dai, H. 2020. Ground movements modeling applying adjusted influence function. *International Journal of Mining Science and Technology* 30(2), pp. 243–249, DOI: 10.1016/j.ijmst.2020.01.007.

Marcak, H. and Pilecki, Z. 2019. Assessment of the subsidence ratio be based on seismic noise measurements in mining terrain. *Archives of Mining Sciences* 64(1), pp. 197–212, DOI: 10.24425/ams.2019.126280.

Meyer et al. 2019 – Meyer, S., Misa, R. and Sroka, A. 2019. *A quantitative description of horizontal ground deformations in the Epe cavern field by using "SubCav" software calculation*. [In:] SMRI Fall 2019 Conference. Berlin, pp. 1–10.

Niedojadło, Z. 2008. The Issue of Copper Deposit Exploitation from Shaft Protective Pillars in LGOM Conditions (*Problematyka eksploatacji złoża miedzi z filarów ochronnych szybów w warunkach LGOM*). *Rozprawy, Monografie* – Akademia Górniczo-Hutnicza im. Stanisława Staszica. AGH Uczelniane Wydawnictwa Naukowo-Dydaktyczne (*in Polish*).

Niedojadło et al. 2014 – Niedojadło, Z., Jura, J., Stoch, T. and Matwij, K. 2014. Horizontal Displacement Modeling in the Knothe-Budryk Theory for LGOM Conditions (*Modelowanie przemieszczeń poziomych w teorii Knothego-Budryka dla warunków LGOM*). *Przegląd Górniczy* 80, pp. 157–164 (*in Polish*).

Niedojadło et al. 2023 – Niedojadło, Z., Stoch, T., Jura, J., Sopata, P., Wójcik, A. and Mrocheń, D. 2023. Monitoring and modelling the deformation state of a dyke of a flotation tailings reservoir of a copper ore mine. *Acta Montan. Slovaca* 28, pp. 123–140, DOI: 10.46544/AMS.v28i1.11.

Nowakowski, A. and Nurkowski, J. 2021. About Some Problems Related to Determination of the E.G. Biot Coefficient for Rocks. *Archives of Mining Sciences* 66, pp. 133–150, DOI: 10.24425/ams.2021.136697.

Polanin et al. 2019 – Polanin, P., Kowalski, A. and Walentek, A. 2019. Numerical Simulation of Subsidence Caused by Roadway System. *Archives of Mining Sciences* 64, pp. 385–397, DOI: 10.24425/ams.2019.128690.

Pöttgens, J.J.E. 1985. Uplift as a result of rising mine waters (*Bodemhebung durch ansteigendes Grubenwasser*). Dev. Sci. art Miner. Surv. Proc. VIth Int. Congr. Mine Surv. Harrogate 2, pp. 928–938 (*in German*).

Preusse, A. and Sroka, A. 2015. Risks posed by rising mine-water levels (*Risiken durch steigende Bergbauwasserstände*). Final Report on Research Project FE no. 0760 0000. Herne (*Unpublished work, in German*).

Puniach et al. 2023 – Puniach, E., Gruszczyński, W., Stoch, T., Mrocheń, D., Ćwiąkała, P., Sopata, P., Pastucha, E. and Matwij, W. 2023. Determination of the coefficient of proportionality between horizontal displacement and tilt change using UAV photogrammetry. *Engineering Geology* 312, DOI: 10.1016/j.enggeo.2022.106939.

Quasnitza, H. 1988. A strategy for calibrating seam motion models and predicting motion elements (*Eine Strategie zur Kalibrierung markschneiderischer Bewegungsmodelle und zur Prädikation von Bewegungselementen*). TU Clausthal (*in German*).

Schmitz, H. 1923. Ground movement processes in mining (*Bodenbewegungsvorgänge im Bergbau*). *Mitteilungen aus dem Marks*. 30, pp. 29–41 (*in German*).

Schober, F. and Sroka, A. 1983. The calculation of ground movements over caverns taking into account the temporal convergence and rock behaviour (*Die Berechnung von Bodenbewegungen über Kavernen unter Berücksichtigung des zeitlichen Konvergenz – und Gebirgsverhaltens*). *Kali und Steinsalz* 8, pp. 352–358 (*in German*).

Schober et al. 1987 – Schober, F., Sroka, A. and Hartmann, A. 1987. A concept for subsidence prediction over cavern fields (*Ein Konzept zur Senkungsvorausberechnung über Kavernenfeldern*). *Kali und Steinsalz* 9, pp. 374–379 (*in German*).

Schutjens et al. 1995 – Schutjens, P.M.T.M., Fens, T.W. and Smits, R.M.M. 1995. Experimental observations of the uniaxial compaction of quartz-rich reservoir rock at stresses of up to 80 MPa. [In:] *Land Subsidence: Proceedings of the Fifth International Symposium on Land SubsidenceBarends*.

Sedlák et al. 2018 – Sedlák, V., Hofierka, J., Gallay, M. and Kaňuk, J. 2018. Specific solution of 3D deformation vector in mine subsidence: A case study of the Košice-Bankov abandoned magnesite mine, Slovakia. *Archives of Mining Sciences* 63(2), pp. 511–531, DOI: 10.24425/122910.

Sheorey et al. 2000 – Sheorey, P.R., Loui, J.P., Singh, K.B. and Singh, S.K. 2000. Ground subsidence observations and a modified influence function method for complete subsidence prediction. *International Journal of Rock Mechanics and Mining Sciences* 37, pp. 801–818, DOI: 10.1016/S1365-1609(00)00023-X.

Sroka, A. 1974. The influence of the advance rate of the mining front on rock mass deformation indicators (*Wpływ prędkości postępu frontu eksploatacji górniczej na wskaźniki deformacji górotworu*). Kraków: AGH *(in Polish)*.

Sroka, A. 1984. Estimation of Some Time-Related Processes in the Rock Mass (*Abschätzung einiger zeitlicher Prozesse im Gebirge*). Im Gebirge. Schriftenreihe Lagerstättenerfassung Und -Darstellung, Bodenbewegungen Und Bergschäden, Ingenieurvermessung. Kolloquium Leoben. pp. 103–132 (*in German*).

Sroka, A. 2011. On the Issue of the Angle Limiting the Extent of Mining-Induced Effects (*Zum Problemdes die Weite der abbaubedingten Einwirkungen begrenzenden Winkels*). [In:] Energie Und Rohstoffe. pp. 312–323 (*in German*).

Sroka et al. 2021 – Sroka, A., Hager, S., Misa, R., Tajduś, K. and Dudek, M. 2021. The application of Knothe's theory for the planning of mining exploitation under the threat of discontinuous deformation of the surface and for the prediction of ground surface movements with rising water levels in the post-mining phase. *Gospodarka Surowcami Mineralnymi – Mineral Resources Management* 37(4), pp. 199–218, DOI: 10.24425/gsm.2021.139737.

Sroka, A. and Hejmanowski, R. 1996. Prediction of Surface Deformation in Room and Pillar Mining: A Case Study of Copper Ore Deposit in LGOM (*Prognozowanie deformacji powierzchni przy eksploatacji filarowo-komorowej na przykładzie złoża rudy miedzi w LGOM*). [In:] XIX Zimowa Szkoła Mechaniki Górotworu. Kraków–Krynica (*in Polish*).

Sroka et al. 2015 – Sroka, A., Knothe, S., Tajduś, K. and Misa, R. 2015. Underground exploitations inside safety pillar shafts when considering the effective use of a coal deposit. *Gospodarka Surowcami Mineralnymi – Mineral Resources Management* 31(3), pp. 93–110, DOI: 10.1515/gospo-2015-27.

Sroka et al. 2018a – Sroka, A., Misa, R. and Tajduś, K. 2018a. Modern applications of the Knothe theory in calculations of surface and rock mass deformations. *Markscheidewesen* 125, pp. 46–53.

Sroka et al. 2018b – Sroka, A., Misa, R. and Tajduś, K. 2018b. Determination of the horizontal deformation factor for mineral and fluidized deposits exploitation. *Acta Geodynamica et Geomaterialia* 15(1), pp. 23–26, DOI: 10.13168/AGG.2017.0030.

Sroka et al. 2017 – Sroka, A., Misa, R., Tajdus, K., Klaus, M., Meyer, S. and Feldhaus, B. 2017. Forecast of rock mass and ground surface movements caused by the convergence of salt caverns for storage of liquid and gaseous energy carriers. [In:] 18. *Geokinematischer Tag.* Freiberg, pp. 34–51.

Sroka, A. and Preusse, A. 2009a. For the Prediction of Flood-Induced Uplifts (*Zur Prognose flutungsbedingter Hebungen*). [In:] 9. Altbergbau-Kolloquium. Montanuniversität Leoben, Leoben, pp. 184–196 (*in German*).

Sroka, A. and Preusse, A. 2009b. *On the prediction of flooding-related ground uplift*. [In:] 9th Colloquium on Abandoned Mines. University of Leoben. pp. 184–196.

Sroka, A. and Schober, F. 1982. The calculation of the maximum ground movements over salt caverns considering the cavity geometry (*Die Berechnung der maximalen Bodenbewegungen über kavernenartigen Hohlräumen unter Berücksichtigung der Hohlraumgeometrie*). *Kali und Steinsalz* 8, pp. 273–277 (*in German*).

Sroka, A. and Schober, F. 1990. Study on the Analysis and Prediction of Ground Subsidence and Compaction Behavior in the Groningen/Ems Estuary Natural Gas Field (*Studie zur Analyse und Vorhersage der Bodensenkungen und des Kompaktionsverhaltens des Erfgasfeldes Groningen/Emsmündung*). (*Unpublished work, in German*).

Sroka et al. 1988 – Sroka, A., Schober, F. and Bartosik-Sroka, T. 1988. Prediction of Rock Movement in Inclined Seam Deposits Considering Anisotropic Rock Properties and the Temporal Convergence and Delay Behavior of the Rock (*Vorausberechnung von Gebirgsbewegungen bei geneigten flözartigen Lagerstätten unter Berücksichtigung anisotroper Gebirgseigenschaften und des zeitlichen Konvergenz- und Verzögerungsverhaltens des Gebirges*). Abschlussbericht zum DFG – Forschungsvorhaben 526 (*Unpublished work, in German*).

Sroka, A. and Tajduś, K. 2009. Calculating Surface Subsidence in Oil and Gas Deposit Exploitation (*Obliczanie osiadania powierzchni terenu przy eksploatacji złóż ropy i gazu*). *Wiertnictwo, Nafta, Gaz* 26, pp. 327–335 (*in Polish*).

Sroka et al. 2022 – Sroka, A., Tajduś, K., Misa, R., Dudek, M. and Mrocheń, D. 2022. Expert Opinion on the Quantification of Ground Movements Expected Due to the Rise of Mine Water in the Water Large Province of Lohberg and Their Relevance for Mining Damage, Especially for the Proper Operation of Sensitive Infrastructure Facilities (*Gutachterliche Stellungnahme zur Quantifizierung der durch den Grubenwasseranstieg in der Wassergroßprovinz Lohberg zu erwartenden Bodenbewegungen und deren Bergschadensrelevanz, insbesondere für den ordnungsgemäßen Betrieb sensibler Infrastruktureinricht*), (*Unpublished work, in German*).

Strzałkowski, P. 2022. Predicting Mining Areas Deformations under the Condition of High Strength and Depth of Cover. *Energies* 15, DOI: 10.3390/en15134627.

Szostak-Chrzanowski et al. 2006 – Szostak-Chrzanowski, A., Chrzanowski, A. and Ortiz, E. 2006. Modeling of ground subsidence in oil fields. *Can. Cent. Geod. Eng.* 9, pp. 133–146.

Tajduś, K. 2015. Analysis of horizontal displacement distribution caused by single advancing longwall panel excavation. *Journal of Rock Mechanics and Geotechnical Engineering* 7(4), pp. 395–403, DOI: 10.1016/j.jrmge.2015.03.012.

Tajduś et al. 2012 – Tajduś, K., Misa, R. and Sroka, A. 2012. Partial Exploitation of Coal Seams with a Special Focus on Pillar Stability and Surface Protection (*Eksploatacja częściowa pokładów węgla ze szczególnym uwzględnieniem stabilności filarów i ochrony powierzchni*). *Górnictwo i Geol.* 7, pp. 212–226 (*in Polish*).

Tajduś et al. 2023 – Tajduś, K., Sroka, A., Dudek, M., Misa, R., Hager, S. and Rusek, J. 2023. Effect of the entire coal basin flooding on the land surface deformation. *Archives of Mining Sciences* 68, pp. 375–391, DOI: 10.24425/ams.2023.146857.

Tajduś et al. 2021 – Tajduś, K., Sroka, A., Misa, R., Tajduś, A. and Meyer, S. 2021. Surface Deformations Caused by the Convergence of Large Underground Gas Storage Facilities. *Energies* 14, DOI: 10.3390/en14020402.

Teeuw, D. 1973. Laboratory Measurement of Compaction Properties of Groningen Reservoir Rock. [In:] *Verhandeligen Kon. Ned. Geol. Mijnbouwk.*

Trojanowski, K. 1970. The Progress of Underground Mining Front and the Rate of Subsidence (*Postęp frontu podziemnej eksploatacji, a prędkość osiadania*). *Przegląd Górniczy* 11 (*in Polish*).

Trojanowski, K. 1973. The Influence of Time Factors and Mining Progress on the Course of Surface Movement Process in the Light of Geodetic Research (*Zagadnienie wpływu czynników czasu i postępu eksploatacji górniczej na przebieg procesu ruchów powierzchni w* świetle *badań geodezyjnych*). *Pr. Kom. Górniczo-Geodezyjnej PAN. Górnictwo* 12 (*in Polish*).

Witkowski et al. 2021 – Witkowski, W.T., Łukosz, M., Guzy, A. and Hejmanowski, R. 2021. Estimation of Mining-Induced Horizontal Strain Tensor of Land Surface Applying InSAR. *Minerals* 11(7), DOI: 10.3390/min11070788.

Zhang et al. 2020 – Zhang, L., Cheng, H., Yao, Z. and Wang, X. 2020. Application of the Improved Knothe Time Function Model in the Prediction of Ground Mining Subsidence: A Case Study from Heze City, Shandong Province, China. *Appl. Sci*. 10, DOI: 10.3390/app10093147.

Zimmermann et al. 2018 – Zimmermann, K., Fritschen, R., Tajduś, K., Sroka, A. and Misa, R. 2018. Subsidence modeling for fluid reservoirs aids hazard mitigation. *Oil and Gas Journal* 116, pp. 46–52.

KNOTHE'S THEORY PARAMETERS – COMPUTATIONAL MODELS AND EXAMPLES OF PRACTICAL APPLICATIONS

Keywords

Knothe's theory, salt caverns, uplift, surface movement, post-mining

Abstract

The theory of Professor Stanislaw Knothe, known as Knothe's Theory, has been the foundation for practical predictive calculations of the impacts of exploitation for many years. It has enabled the large-scale extraction of coal, salt and metal ores located in the protective pillars of cities and prime surface structures. Knothe's Theory has been successfully applied in Polish and global mining for over seventy years, making it one of the most well-known and recognized achievements in Polish mining science. Knothe's Theory provides a temporal-spatial description of subsidence that relies on four essential parameters: the vertical scale parameter a, the horizontal displacement parameter λ, the horizontal range scale parameter $cot\beta$ and the time scale parameter c.

This article characterizes the parameters of Knothe's Theory used in various current applications for calculating subsidence, surface and rock uplift, and other applications of the theory, even beyond its classical form. The presented solutions are based on a mathematical model of the interaction of a complex element and cover topics such as subsidence during full exploitation with roof collapse and full exploitation with backfilling, pillar-room mining, the effect of salt caverns on the surface and salt rock, and fluid deposits and surface uplift caused by changes in the water level within closed coal mines. The article also discusses the evolution of the range angle of the main influences and presents Knothe's solutions related to time, describing the horizontal displacement parameter λ.

PARAMETRY TEORII KNOTHEGO – MODELE OBLICZENIOWE I PRZYKŁADY PRAKTYCZNEGO ZASTOSOWANIA

Słowa kluczowe

teoria Knothego, kawerny solne, wypiętrzenie powierzchni terenu, przemieszczenia powierzchni, problemy pogórnicze

Streszczenie

Teoria Profesora Stanisława Knothego zwana teorią Knothego jest od wielu lat podstawą do praktycznych obliczeń prognostycznych wpływów eksploatacji, a tym samym umożliwiła podjęcie na szeroką skalę wydobycia dużych zasobów węgla, soli i rud metali znajdujących się m.in. w filarach ochronnych miast i ważnych obiektów na powierzchni. Teoria Knothego jest z powodzeniem stosowana w polskim i światowym górnictwie od ponad siedemdziesięciu lat. Jest ona jednym z najlepiej znanych i uznanych na świecie osiągnięć polskiej nauki górniczej. Do czasoprzestrzennego opisu osiadania wg teorii Knothego konieczna jest znajomość wartości czterech podstawowych parametrów: parametru skali pionowej a, parametru skali zasięgu poziomego $cot\beta$, parametru przemieszczenia poziomego λ oraz parametru skali czasu c.

W artykule scharakteryzowano parametry teorii Knothego stosowane przy różnych wykorzystywanych aktualnie zastosowaniach teorii Knothego do obliczania m.in. osiadania oraz podnoszenia powierzchni i górotworu oraz innych zastosowań teorii, również poza jej klasyczną formą. Przedstawione rozwiązania bazują na matematycznym modelu oddziaływania elementu złożowego i dotyczą, m.in. osiadania przy eksploatacji pełnej z zawałem stropu oraz eksploatacji pełnej z podsadzką, eksploatacji filarowo-komorowej, wpływu kawern solnych na powierzchnię i górotwór solny. W pracy poruszono także kwestię złóż fluidalnych oraz podnoszenia powierzchni terenu spowodowanego zmianą poziomu wód kopalnianych w obrębie zamkniętych kopalń węgla kamiennego a także opisano ewolucję kąta zasięgu wpływów głównych oraz przedstawiono rozwiązania Knothego związane z czasem i opisano parametr przemieszczenia poziomego λ.